RADIATION AND RESIDUAL DOSE RATE INDUCED BY THE BEAM LOSS AT VARIOUS INJECTION ENERGIES

N. Nakao, Y. Irie, M. Uota, M. Shirakata, KEK, 1-1 Oho, Tsukuba, Ibaraki 305-0801, Japan
N. Mokhov, A. Drozhin, Fermilab., P.O.Box 500, Batavia, IL 60510-0500, USA

Abstract

Hadron cascade simulation was performed with the Monte Carlo code, MARS, using the beam loss distributions calculated by the multi-turn tracking Monte Carlo code, STRUCT, for primary-proton energies of 200, 400, 600 and 1000 MeV. Distributions of secondary particle flux, absorbed dose and residual dose at the accelerator components induced by the beam loss at a synchrotron injection part were estimated and their energy dependences were clarified.

1 INTRODUCTION

On an accelerator design, estimations of absorbed dose and residual activity induced by beam loss are very important to know radiation damages of the accelerator components and instruments, and to reduce external exposures for workers during hands-on-maintenance.

In this work, the calculation of beam loss distribution along the proton synchrotron ring was performed by the STRUCT code [1], and the hadron cascade induced by the beam loss was simulated by the MARS code [2]. In this continuous Monte Carlo calculation, absorbed dose and contact-dose-equivalent rate of accelerator components due to the beam loss were estimated, and their energy dependences from 200 to 1000 MeV were clarified for a radiation protection purpose.

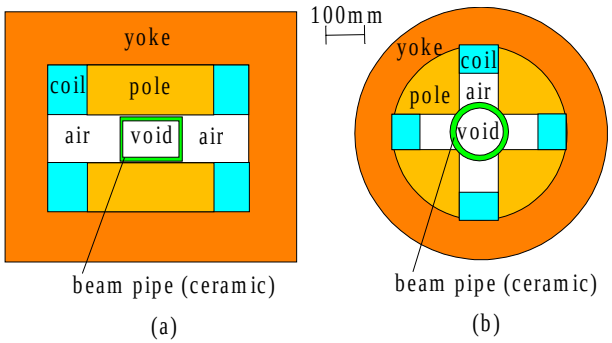

Figure 1: Cross sectional views of (a) dipole- and (b) quadrupole-magnet geometries used in the MARS calculation (parpendicular to the beam orbit).

2 CALCULATION

2.1 STRUCT calculation

Using the multi-turn tracking Monte Carlo code, STRUCT [1], primary protons of beam halo were traced along a whole synchrotron ring of 350 meter [3]. Inner structure geometries of beam pipe and collimator along the orbit and magnetic fields at magnet regions were taken into account in the calculation. If the particles go out of the boundary and/or lose more than 30% of primary-kinetic energy, the traces are terminated and the positions, directions and kinetic energies of the lost particles are stored for the MARS calculation. In this work, primary-proton energies of 200, 400, 600 and 1000 MeV were employed, and the beam loss distributions along the ring were calculated with 5,000 primary protons.

2.2 MARS calculation

Hadron cascade and radiation transmission in the materials along a 100-meter path of the collimator region around the injection of the ring were calculated by the Monte Carlo code, MARS [2]. The lost protons in the STRUCT calculation started their histories with their given positions, directions and kinetic energies.

All ring modules such as magnets, collimators, scrapers and beam pipes were taken into account as calculation ge-

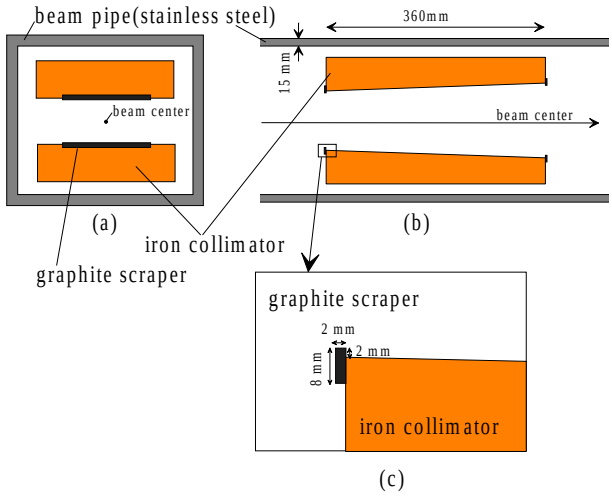

Figure 2: Cross-sectional views of a horizontal-collimator region for (a) perpendicular and (b) parallel plane to the beam orbit, and (c) an enlargement of the graphite scraper attached to the primary-collimator edge.

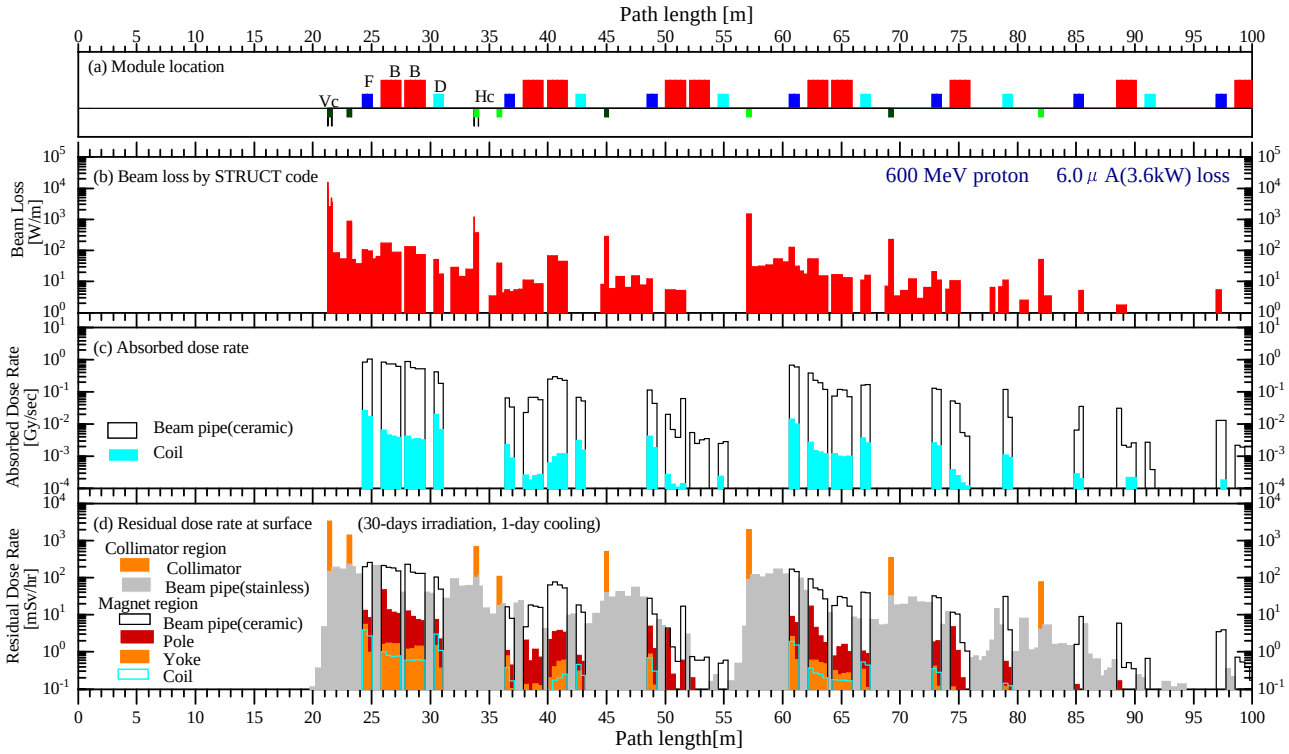

Figure 3: Distributions along the 100 m path of the injection part in the case for 600 MeV protons. (a) Module location(Vc:vertical collimator, F:focusing magnet, B:bending magnet, D:defocusing magnet, Hc:horizontal collimator), (b) beam loss calculated by the STRUCT code, (c) absorbed-dose rate of ceramic and coil, and (d) residual-dose rate at component surfaces.

ometries. In order to save calculation time, geometries of dipole and quadrupole magnets were simplified as shown in the Fig. 1. Rectangular- and cylindrical-ceramic beam pipes of 15-mm thickness were used for the dipole- and quadrupole-magnet regions, respectively. A natural copper is used for the coil region, and a natural iron for the yoke and the pole regions. On the other hand, in a drift space region, a rectangular stainless steel of 15-mm thickness was used for a beam pipe. Fig. 2 shows cross sectional views of a horizontal collimator region. Several iron collimators of 360-mm length were equipped inside the stainless beam pipe to scrape the beam halo horizontally or vertically. The inner surface of the collimator follows the beam envelope with beam emitance, 312 mm mrad, and $\Delta p/p = \pm 0.5\%$. Graphite scrapers of 2-mm thickness were attached at the front and rear edges of the primary collimator as shown in the Fig. 2(c) to scatter the beam halo.

2D-magnetic fields were calculated with the POISSON code, and were taken into account at the magnet regions. Total energy depositions by the proton beam loss were normalized to 3.6 kW for all the injection energies.

The distributions of particle flux, absorbed-dose rate and residual-dose rate were estimated with the MARS code. In this work, the residual-dose rate indicates a contact-dose-equivalent rate due to the residual activity at a material surface after 30-days operation (irradiation) and 1-day cooling. In order to see detailed distributions of these quantities, drift spaces were divided into every 40∼50 cm, and a quadrupole magnet of 80-cm length and a dipole magnet of 167-cm length were divided into 2 and 4 parts, respectively.

3 RESULTS AND DISCUSSIONS

Fig. 3(a) shows module locations along the 100 m path around the collimator region of the ring. A beam loss distribution for 600-MeV protons calculated by the STRUCT code is shown in Fig. 3(b). Absorbed-dose rates of ceramic beam pipe and coil were estimated with the energy depositions calculated by MARS code, and are shown in Fig. 3(c). The highest absorbed-dose rates and their annual values for all energies are tabulated in Table 1(a), on the assumptions of a total beam loss of 3.6 kW and an operation time of 5000 hours per year. Absorbed-dose rate normalized to unit beam loss (1 W/m) were also estimated and tabulated in the Table 1(b). Distribution of residual-dose rate at various accelerator components was calculated by MARS code, and is shown in Fig. 3(d).

Energy dependences of particle flux, absorbed-dose rate and residual-dose rate at several parts of the primary collimator, the focusing magnet and the bending magnet are shown in Figs. 4, 5 and 6, respectively. The collimators equipped inside the beam pipe are considered to be activated mainly by the primary beam halo, and the residual-dose rates for the various energies were almost constant as shown in Fig. 4.

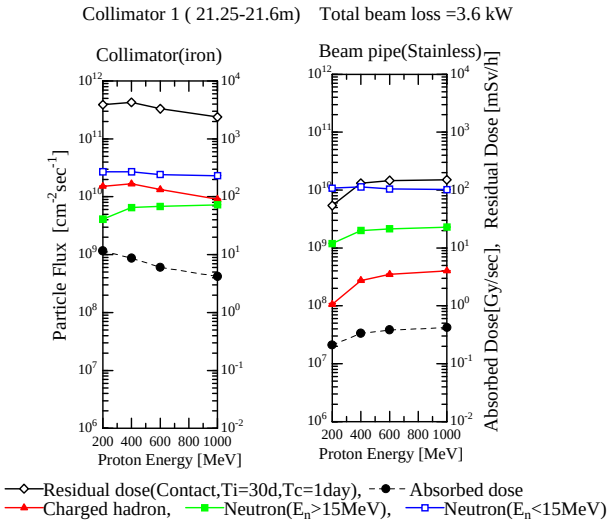

Figure 4: Energy dependences of particle flux, absorbed-dose rate and residual-dose rate at the primary collimator (21.25-21.6m).

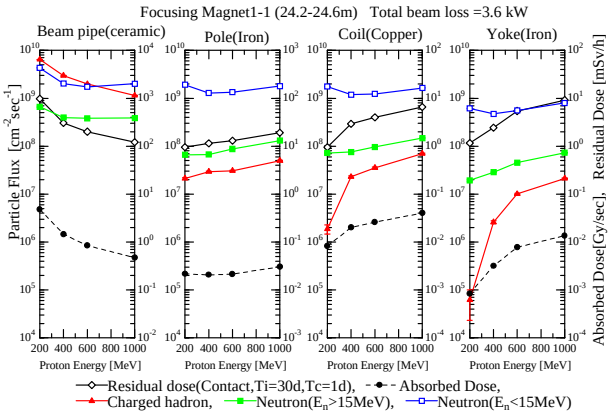

Figure 5: Energy dependences of particle flux, absorbed-dose rate and residual-dose rate at the focusing magnet(24.2-24.6m).

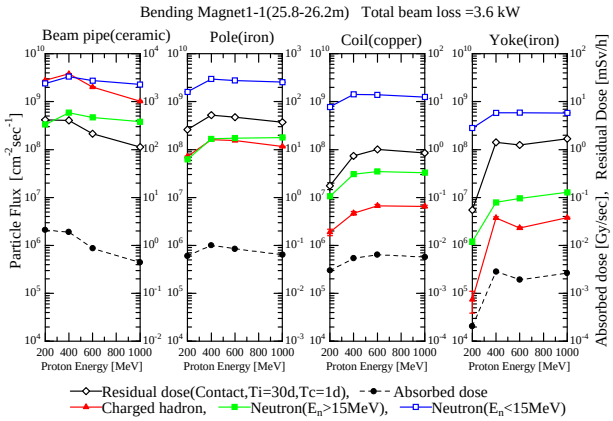

Figure 6: Energy dependences of particle flux, absorbed-dose rate and residual-dose rate at the bending magnet(25.8-26.2m).

Table 1: (a) Maximum absorbed-dose rates for ceramic beam pipe and their annual values, and (b) averaged absorbed-dose rate per beam loss for ceramic and coil of quadrupole and bending magnets.

material	unit	Proton Energy [MeV] 200	400	600	1000
(a) ceramic	Gy/sec	4.8	1.9	1.0	0.62
	Gy/yr.	8.7E7*	3.4E7	1.9E7	1.1E7
(b) ceramic	Gy/sec	1.5E-2	1.2E-2	8.8E-3	6.5E-3
coil(Quad)	per	5.7E-5	1.6E-4	3.0E-4	3.6E-4
coil(Bend)	W/m	2.5E-5	3.2E-5	4.2E-5	6.0E-5

* Read as 8.7×10^{7}

It can be seen that the absorbed dose and the residual dose at the ceramic beam pipe decrease with increasing the primary-proton energy, as shown in Figs. 5 and 6. On the other hand, those at the coil and the yoke in outer regions increase with increasing the primary-proton energy, especially, a rapid increase can be seen between 200 and 600 MeV because higher energy particles can deposit their energies to farther materials due to hadron-cascade development.

4 CONCLUSION

Hadron cascade induced by the beam loss was simulated with the MARS code. The beam loss distributions were calculated with the STRUCT code for primary-proton energies were 200, 400, 600 and 1000 MeV. If the total power of beam loss at injection is kept constant for all injection energies, it is found that lower injection energy is preferable from the view point of radiation protection. Absorbed doses for accelerator modules are also estimated, which can be useful for material selection by their radiation hardness.

REFERENCES

[1] I. Baishev et al., SSCL-MAN-0034, (1994).

[2] N. V. Mokhov et al., FERMILAB-Conf-98/379 (1998).

[3] M. Shirakata, Y. Irie, M. Uota, N. Nakao, A. Drozhin and N. V. Mokhov, “Estimations on the Beam Halo Collection at the High Intensity Accelerator”, EPAC2000, this proceedings.